Supporting Information

Collignon et al. 10.1073/pnas.1013928108

SI Text

Behavioral Results. As expected, because of the use of a staircase paradigm, no difference of performance was observed between groups or between tasks (Fig. S1 *B* and *C*). Moreover, the simple ANOVA testing the group effect on auditory–spatial and auditory–pitch resolution level did not show a significant between-group effect (Fig. S1*D*). In the pitch discrimination task, the mean distance between the probe (1,000 Hz, central position) and the target was 27 Hz (±17 Hz SD) in the sighted group and 16 Hz (±20 Hz) in the blind group. In the spatial discrimination task, the mean distance between the probe (1,000 Hz, central position) and the target was 276 μs interaural time difference (ITD) and 2.76% interaural level difference (ILD) (± 198 μs ITD and 1.98% ILD) in the sighted group and 284 μs ITD and 2.84% ILD (±196 μs ITD and 1,96% ILD) in the blind group.

The lack of performance differences between the two groups may seem puzzling at a first glance, especially regarding the spatial task because several previous studies outlined superior performance of the congenitally blind (CB) over sighted individuals (SI) for this ability (see ref. 1 for a recent review on the topic). However, previous studies showing difference in performance between CB and SI groups in spatial tasks have demonstrated that such differences manifest when sounds are presented monaurally (2, 3) or in the periphery (4). In the present experiment, the spatial task required the lateralization of intracranial sounds perceived along a line joining the two ears (*Materials and Methods*, main text). These sounds lead to a near-centered intracranial perceived location, roughly estimated to the foveal–parafoveal border if we attempt to make a correspondence with 3D sounds (5). This strongly suggests that blind individuals use subtle spatial cues more efficiently than sighted controls, particularly the spectral content of the sound, which is one of the principal remaining cues for localizing a source under a monaural listening condition or for the localization of sounds in the periphery (6). However, in the present experiment intracranial sound locations were obtained by jointly adjusting the ITD and ILD of pure tone. No head-related transfer function, which includes spectral cues, was used because people only had to judge the location of sounds along the azimuth coordinate. Indeed, our absence of better performance in the CB group may be related to this absence of spectral content in the sounds used in the present experiment.

Functional MRI Analysis. The analysis of functional MRI (fMRI) data, based on a mixed-effects model, was conducted in two serial steps, accounting respectively for fixed and random effects. For each subject, changes in brain regional responses were estimated by a general linear model including the responses to the pitch and spatial conditions. These regressors consisted of boxcar function convolved with the canonical hemodynamic response function. The instruction preceding each block, movement parameters derived from realignment of the functional volumes (translations in x, y, and z directions and rotations around x, y, and z axes) and a constant vector were also included as covariates of no interest. High-pass filtering was implemented in the design matrix using a cutoff period of 128 s to remove slow drifts from the time series. Serial correlations in fMRI signal were estimated using an autoregressive (order 1) plus white-noise model and a restricted maximum likelihood algorithm.

Linear contrasts tested the main effect of each condition ([Pitch], [Spatial], [Spatial > Pitch], and [Pitch > Spatial]) and the main effect of general auditory processing ([Spatial + Pitch]) and generated statistical parametric maps [SPM(T)]. These summary statistics images were then further spatially smoothed (Gaussian kernel 6 mm FWHM) and entered in a second-level analysis, corresponding to a random-effects model, accounting for intersubject variance. One-sample *t* tests characterized the main effect of conditions ([Pitch], [Spatial], [Spatial > Pitch], and [Pitch > Spatial]) in SI and CB groups separately. A conjunction analysis based on a conjunction null hypothesis characterized brain areas jointly activated for the contrasts [Spatial > Pitch] and [Pitch > Spatial] in both groups (CI and SI). Two-sample *t* tests were then performed to identify group effects independent of the condition ([CB > SI] × [Spatial + Pitch]) and to explore group × condition interaction effects ([CB > SI] × [Pitch > Spatial] and [CB > SI] × [Spatial > Pitch]). Two-sample *t* tests were also performed to investigate group effect for each condition separately ([CB > SI] × [Spatial]; [CB > SI] × [Pitch]; [SI > CB] × [Spatial]; [SI > CB] × [Pitch]; see Table S5). Main effects of condition in each group were used as inclusive or exclusive masks to identify which group was driving the interaction effects.

The resulting set of voxel values for each contrast constituted a map of the *t* statistic [SPM(T)], thresholded at $P < 0.001$ (uncorrected for multiple comparisons; Z threshold of 3.09). Statistical inferences were performed at a threshold of $P < 0.05$ after correction for multiple comparisons over either the entire brain volume or over small spherical volumes (10-mm radius), located in structures of interest. Significant clusters were anatomically labeled using structural neuroanatomy information and probabilistic cytoarchitectonic maps provided in Anatomy Toolbox 1.7b (7) or using a brain atlas for brain regions not covered by this toolbox (8).

Psychophysiological interaction (PPI) analyses (9) were computed to identify any brain regions showing a significant change in the functional connectivity with a seed region (the right cuneus, the right middle occipital gyrus, the right middle occipitotemporal gyrus, and the right lingual gyrus) as a function of the experimental condition ([Spatial, Pitch]) in the CB group. Indeed, PPI analyses were conducted to test the hypothesis that functional connectivity between seed regions and the rest of the brain not only differed between conditions (Spatial vs. Pitch) but was also influenced by the experimental group (CB or SI). In each individual, time-series of activity from the seed area were extracted from the local maxima detected within 10 mm of the peaks identified in the [CB > SI] × [Spatial > Pitch] contrast. New linear models were generated at the individual level, using three regressors. One regressor represented the condition (Spatial > Pitch). The second regressor was the activity extracted in the reference area. The third regressor represented the interaction of interest between the first (psychological) and the second (physiological) regressor. To build this regressor, the underlying neuronal activity was first estimated by a parametric empirical Bayes formulation, combined with the psychological factor and subsequently convolved with the hemodynamic response function (10). The design matrix also included movement parameters. A significant PPI indicated a change in the regression coefficients between any reported brain area and the reference region, related to the experimental condition (Spatial > Pitch) in CB. Next, individual summary statistic images obtained at the first level (fixed-effects) analysis were spatially smoothed (6-mm FWHM Gaussian kernel) and entered in a second-level (random-effects) analysis using a one-sample *t* test. Inferences were conducted as for the main-effect analysis. PPI carried out in the SI with the same seed areas were used as exclusive masks ($P = 0.05$) to ensure that the pattern of functional connectivity with the seeds

areas that is present in CB is not present in SI. These analyses allow exploration of the functional connectivity between any seed area and the rest of the brain, in CB, during Spatial sound processing compared with Pitch processing.

Finally, in the random-effects analyses, posterior probability maps (PPMs) enabling conditional or Bayesian inferences about regionally specific effects were performed (11). PPMs represent a powerful complementary approach to classic statistical parametric maps inferences (11). This type of analysis allows controlling that one seed area activated in one group (CB) presents a low probability of activation in the other group (SI). This is of particular interest in the case of the present study because it gives a direct measurement of the intrinsic probability of activation in SI of regions showing significantly more activity in CB than SI. PPMs and effect size were computed for the contrasts [Spatial + Pitch] and [Spatial > Pitch] in the CB group to verify that seed areas (using 10-mm volume of interest around activation peaks) obtained with [CB > SI] in these contrasts (the right middle occipital gyrus, the left calcarine gyrus, and the left middle occipital gyrus for [Spatial+Pitch]; the right cuneus, the right middle occipital gyrus, and the right lingual gyrus for [Spatial > Pitch]) have a low probability of activation in the SI group.

Coordinates of Areas of Interest Used for Spherical Small-Volume Corrections. Literature reporting brain activations related to auditory–pitch or auditory–spatial processing in blind and sighted subjects was considered for selecting coordinates of interest, depending of the contrast of interest. Before performing any small-volume correction (svc), peaks reported in Talairach (Talairach and Tournoux, 1988) space were transformed to Montreal Neurological Institute space using Matthew Brett's bilinear transformation (http://imaging.mrc-cbu.cam.ac.uk/imaging/MniTalairach; no coordinates were shifted more than 5 mm). Standard stereotactic coordinates of previously published a priori locations, used for spherical svc, are as follows:

Frontal locations.

Right superior frontal gyrus: 3, 2, 52 (12), 34, −2, 36 (13), 36, 0, 40 (13); frontal eye fields: x right from 20 to 41, left from −40 to −18; y from −17 to 11; z from 40 to 61 (14, 15); right middle frontal gyrus: 48, 34, 28 (16), 30, 50, 20 (16), 44, 16, 28 (17); left middle frontal gyrus: −38, 52, 10 (16), −42, 44, −2 (17); right inferior frontal gyrus: 48, 11, 04 (12), 34, 28, −02 (16).

Parietal locations.

Bilateral inferior parietal lobule: 66, −26, 26 (18), 42, −43, 48 (18), 50, −33, 47 (19), 46, −44, 36 (13), 42, −43, 48 (20), 61, −27 44 (21), −52, −24, 36 (13), 25, −45, 39 (22); right intraparietal sulcus: 42, −43, 48 (20); right superior parietal lobule: 26, −66, 54 (17), right precuneus: 8, −55, 60 (17).

Temporal locations.

Right posterior superior temporal gyrus: 62, −25, 3 (23), 60, −21, 2 (22); right middle temporal gyrus: −56, −19, −5 (24), 44, −72, −2 (25); right inferior temporal region: 57, −07, −25 (21); left superior temporal gyrus: −53, −20, 06 (22), −40, −32, 12 (26); left middle temporal gyrus: −37, −25, 05 (22); left planum polare: −48, −6, −14 (27).

Insula.

Left insula: −42, 2, 10 (28), −30, 20, 10 mm (29), −36, −18, 18 (30), −29, −3, 18 (30).

Putamen.

Left putamen: −22, 0, 11 (30).

Occipital locations.

Right middle lateral occipito-temporal gyrus: 48, −56, 6 (25), 46, −64, 17 (3), 44, −77, −2 (31); right cuneus: 22, −76, 24 (32), 24, −76, 24 (33), 3, −83, 12 (3); right lingual gyrus: 15, −73, −6 (3), 40, −68, −4 (32); right occipito-parietal junction: 12, −76, 37 (34).

Cerebellum.

Right cerebellum: 15, −64, −50 (35), 30, −54, −15 (30); left cerebellum: −20, −59, −21 (30).

1. Collignon O, Voss P, Lassonde M, Lepore F (2009) Cross-modal plasticity for the spatial processing of sounds in visually deprived subjects. *Exp Brain Res* 192:343–358.
2. Lessard N, Paré M, Lepore F, Lassonde M (1998) Early-blind human subjects localize sound sources better than sighted subjects. *Nature* 395:278–280.
3. Gougoux F, Zatorre RJ, Lassonde M, Voss P, Lepore F (2005) A functional neuroimaging study of sound localization: Visual cortex activity predicts performance in early-blind individuals. *PLoS Biol* 3:e27.
4. Röder B, et al. (1999) Improved auditory spatial tuning in blind humans. *Nature* 400: 162–166.
5. Blauert J (1997) *Spatial Hearing: The Psychophysics of Human Sound Localization* (MIT Press, Cambridge, MA).
6. Van Wanrooij MM, Van Opstal AJ (2004) Contribution of head shadow and pinna cues to chronic monaural sound localization. *J Neurosci* 24:4163–4171.
7. Eickhoff SB, et al. (2007) Assignment of functional activations to probabilistic cytoarchitectonic areas revisited. *Neuroimage* 36:511–521.
8. Mai J, Patxinos G, Voss T (2007) *Atlas of the Human Brain* (Elsevier, New York), 3rd Ed.
9. Friston KJ, et al. (1997) Psychophysiological and modulatory interactions in neuroimaging. *Neuroimage* 6:218–229.
10. Gitelman DR, Penny WD, Ashburner J, Friston KJ (2003) Modeling regional and psychophysiologic interactions in fMRI: The importance of hemodynamic deconvolution. *Neuroimage* 19:200–207.
11. Friston KJ, Penny W (2003) Posterior probability maps and SPMs. *Neuroimage* 19: 1240–1249.
12. Rämä P, et al. (2004) Dissociable functional cortical topographies for working memory maintenance of voice identity and location. *Cereb Cortex* 14:768–780.
13. Weeks RA, et al. (1999) A PET study of human auditory spatial processing. *Neurosci Lett* 262:155–158.
14. Paus T (1996) Location and function of the human frontal eye-field: A selective review. *Neuropsychologia* 34:475–483.
15. Garg A, Schwartz D, Stevens AA (2007) Orienting auditory spatial attention engages frontal eye fields and medial occipital cortex in congenitally blind humans. *Neuropsychologia* 45:2307–2321.
16. Poirier C, et al. (2005) Specific activation of the V5 brain area by auditory motion processing: An fMRI study. *Brain Res Cogn Brain Res* 25:650–658.
17. Bushara KO, et al. (1999) Modality-specific frontal and parietal areas for auditory and visual spatial localization in humans. *Nat Neurosci* 2:759–766.
18. Griffiths TD, et al. (1998) Right parietal cortex is involved in the perception of sound movement in humans. *Nat Neurosci* 1:74–79.
19. Zatorre RJ, Bouffard M, Belin P (2004) Sensitivity to auditory object features in human temporal neocortex. *J Neurosci* 24:3637–3642.
20. Voss P, Gougoux F, Zatorre RJ, Lassonde M, Lepore F (2008) Differential occipital responses in early- and late-blind individuals during a sound-source discrimination task. *Neuroimage* 40:746–758.
21. Maeder PP, et al. (2001) Distinct pathways involved in sound recognition and localization: a human fMRI study. *Neuroimage* 14:802–816.
22. Alain C, Arnott SR, Hevenor S, Graham S, Grady CL (2001) "What" and "where" in the human auditory system. *Proc Natl Acad Sci USA* 98:12301–12306.
23. Zatorre RJ, Evans AC, Meyer E (1994) Neural mechanisms underlying melodic perception and memory for pitch. *J Neurosci* 14:1908–1919.
24. Kiehl KA, Laurens KR, Duty TL, Forster BB, Liddle PF (2001) Neural sources involved in auditory target detection and novelty processing: an event-related fMRI study. *Psychophysiology* 38:133–142.
25. Poirier C, et al. (2006) Auditory motion perception activates visual motion areas in early blind subjects. *Neuroimage* 31:279–285.
26. Poeppel D, et al. (2004) Auditory lexical decision, categorical perception, and FM direction discrimination differentially engage left and right auditory cortex. *Neuropsychologia* 42:183–200.
27. Barrett DJ, Hall DA (2006) Response preferences for "what" and "where" in human non-primary auditory cortex. *Neuroimage* 32:968–977.
28. Hall DA, Plack CJ (2009) Pitch processing sites in the human auditory brain. *Cereb Cortex* 19:576–585.
29. Renier LA, et al. (2009) Multisensory integration of sounds and vibrotactile stimuli in processing streams for "what" and "where". *J Neurosci* 29:10950–10960.
30. Peck KK, et al. (2009) Event-related functional MRI investigation of vocal pitch variation. *Neuroimage* 44:175–181.
31. Tootell RB, et al. (1995) Functional analysis of human MT and related visual cortical areas using magnetic resonance imaging. *J Neurosci* 15:3215–3230.
32. Weeks R, et al. (2000) A positron emission tomographic study of auditory localization in the congenitally blind. *J Neurosci* 20:2664–2672.
33. Haxby JV, et al. (1994) The functional organization of human extrastriate cortex: A PET-rCBF study of selective attention to faces and locations. *J Neurosci* 14:6336–6353.
34. Weaver KE, Stevens AA (2007) Attention and sensory interactions within the occipital cortex in the early blind: an fMRI study. *J Cogn Neurosci* 19:315–330.
35. Zimmer U, Lewald J, Erb M, Grodd W, Karnath HO (2004) Is there a role of visual cortex in spatial hearing? *Eur J Neurosci* 20:3148–3156.
36. Oldfield RC (1971) The assessment and analysis of handedness: The Edinburgh inventory. *Neuropsychologia* 9:97–113.

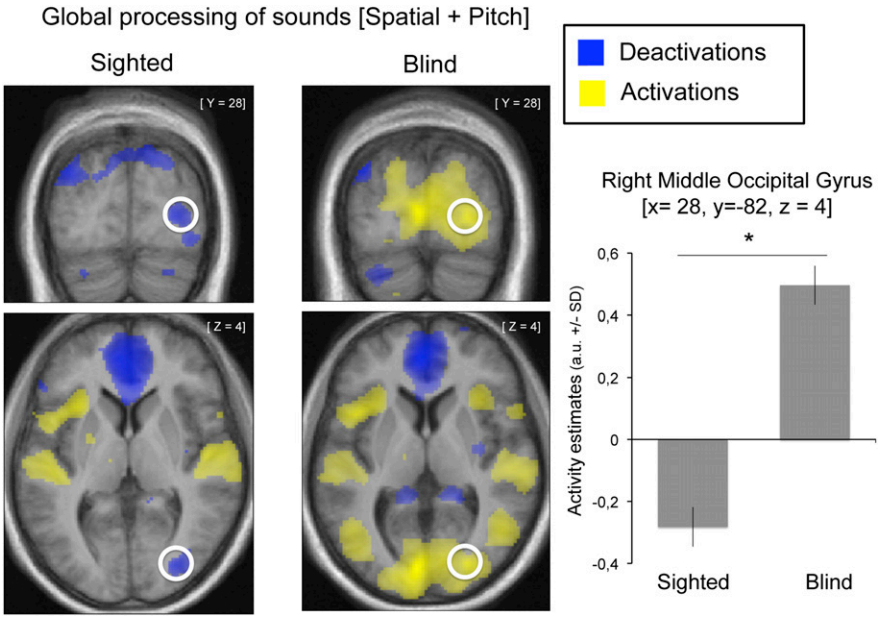

Fig. S1. Activations (yellow) and deactivations (blue) obtained on contrasts testing the main effects of global sound processing [Spatial + Pitch] in both groups separately. Functional data are displayed ($P_{uncorrected} < 0.001$) over coronal and horizontal sections of the mean structural image of all blind subjects and of all sighted subjects respectively normalized to the same stereotactic space. *Right:* Mean activity estimates (arbitrary unit ± SEM) associated with sound processing [Spatial + Pitch] in the sighted and the blind groups for peak activation and peak deactivation estimates in the right middle occipital gyrus in both groups separately. One can see that this region is strongly activated in blind subjects, whereas it shows deactivation in sighted subjects.

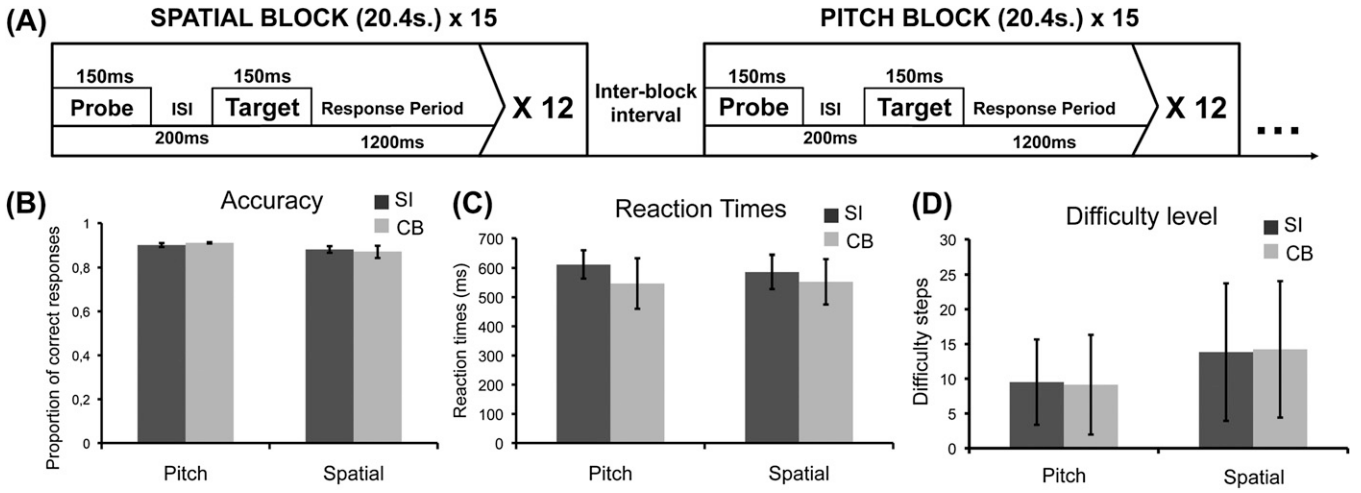

Fig. S2. Experimental design and behavioral results. (*A*) fMRI acquisition design. Performance in the scanner is illustrated by the accuracy scores (*B*) and the reaction times (*C*) in both tasks, as well as by the spatial and the pitch difficulty level (*D*) of these tasks. No between-group or between-task effects were found to be significant.

Table S1. Functional results for the main effect of condition ([Pitch > Spatial] and [Spatial > Pitch]) in conjunction in each group (SI and CB)

Area	Cluster size	*x* (mm)	*y* (mm)	*z* (mm)	*Z*	*P*
Conjunction [CB ∩ SI] × [Spatial − Pitch]						
R superior frontal gyrus	1,308	32	0	48	5.34	0.002*
R middle occipito-temporal gyrus	690	48	−54	10	5.31	0.000
R inferior parietal lobule	1,444	52	−40	30	4.95	0.005
R middle frontal gyrus	340	40	56	16	4.29	0.001
R precuneus-superior parietal lobule	385	4	−52	60	4.23	0.001
L inferior frontal gyrus	64	−40	50	−6	3.58	0.01
R insula–R inferior frontal gyrus	107	46	22	−8	3.54	0.024
R middle frontal gyrus	32	44	06	30	3.30	0.025
Conjunction [CB ∩ SI] × [Pitch − Spatial]						
R anterior inferior temporal gyrus	35	44	0	−32	4.24	0.024
L anterior planum polare	405	−24	4	−20	4.15	0.013
L inferior frontal gyrus/insula	90	−46	06	04	4.12	0.002
L posterior middle temporal gyrus	207	−42	−36	02	4.12	0.006
L precentral gyrus	75	−38	−24	66	3.41	0.016
L middle temporal gyrus	21	−48	−22	−12	3.31	0.034

Brain activations significant after correction over the entire volume (*) or over small volume of interest (svc). R, right; L, left.

Table S2. Summary of the PPI analyses (functional connectivity analyses) performed on the [Spatial > Pitch] contrast in CB

Seed area for PPI analyses in CB	Cluster size	*x* (mm)	*y* (mm)	*z* (mm)	*Z*	*P*
Right cuneus						
R superior frontal gyrus	31	18	−12	60	3.87	0.005
	—	22	−18	70	3.26	0.028
L superior frontal gyrus	84	−14	−10	64	3.86	0.006
R inferior parietal lobule	25	58	−30	54	3.49	0.021
	—	64	−24	46	3.26	0.027
R middle frontal gyrus	7	56	22	36	3.45	0.037
L inferior parietal lobule	34	−64	−24	40	3.34	0.028
L inferior parietal lobule	7	−66	−22	30	3.23	0.029
R middle frontal gyrus	1	50	38	26	3.13	0.037
R inferior parietal lobule	1	30	−38	40	3.11	0.038
Right lateral occipital gyrus						
R inferior parietal lobule	29	32	−38	38	3.71	0.013
L superior frontal gyrus	66	−16	−12	58	3.70	0.010
R cuneus	42	14	−84	38	3.58	0.014
R cerebellum	17	14	−72	−44	3.26	0.027
Right middle occipito-temporal gyrus						
R inferior frontal gyrus	14	52	10	6	3.24	0.026
R superior frontal gyrus	6	6	6	60	3.21	0.028
R supramarginal gyrus	8	36	−40	42	3.18	0.030
Right lingual gyrus						
R inferior parietal lobule	26	32	−34	42	3.4	0.038

Brain activations significant after correction over small volume of interest (svc). All of the clusters reported in the table are not affected by an exclusive mask ($P = 0.05$) of the PPI carried out in the sighted subjects with the same seeds areas, further indicating that the reported regions present a pattern of functional connectivity with the seeds areas that is present on CB but not on SI. R, right; L. left.

Table S3. Small-volume correction analysis done around the Montreal Neurological Institute coordinate 44, −77, −2, identified as hMT+/V5 by Tootel et al. (1) and coordinate 24, −76, 24, identified as a visuospatial region by Haxby et al. (2)

		Coordinates				
Subjects	Cluster size	*x* (mm)	*y* (mm)	*z* (mm)	*Z*	*P*
hMT+/V5 (44, −77, −2)						
CB1	8	46	−66	−12	3.56	0.041
CB2	629	44	−72	12	>8	0.000
CB3	1,255	44	−66	−2	>8	0.000
CB4	42	48	−66	8	4.32	0.003
CB5	4	52	−64	2	4.16	0.007
CB6	—	—	—	—	—	—
CB7	249	36	−76	−10	4.86	0.000
CB8	48	40	−76	−2	3.82	0.021
CB9	245	48	−74	12	4.26	0.004
CB10	27	52	−70	8	4.2	0.004
CB11	—	—	—	—	—	—
V3/V3A (24, −76, 24)						
CB1	264	22	−84	34	5.53	0.000
CB2	678	18	−70	34	6.72	0.000
CB3	1305	24	−86	20	>8	0.000
CB4	4	28	−78	38	3.46	0.05
CB5	673	24	−84	36	7.25	0.000
CB6	—	—	—	—	—	—
CB7	260	16	−74	26	5.45	0.000
CB8	40	32	−88	22	3.57	0.000
CB9	372	38	−80	26	5.76	0.000
CB10	176	36	−82	18	5.3	0.000
CB11	48	22	−66	16	3.67	0.033

Brain activations significant after correction over small spherical volume of interest (15-mm radius), centered on the above-mentioned coordinates.

1. Tootell RB, et al. (1995) Functional analysis of human MT and related visual cortical areas using magnetic resonance imaging. *J Neurosci* 15:3215–3230.
2. Haxby JV, et al. (1994) The functional organization of human extrastriate cortex: A PET-rCBF study of selective attention to faces and locations. *J Neurosci* 14:6336–6353.

Table S4. Characteristics of the blind subjects

Subject	Age (y)	Sex	Hand	Residual visual perception	Onset	Cause of blindness	Education	Musical experience
CB1	32	F	R	No	0	Glaucoma	High school	No
CB2	43	M	R	No	0	Glaucoma	University	Yes
CB3	39	M	R	Diffuse light	0	Leber's congenital amaurosis	University	No
CB4	56	F	R	No	0	Retinopathy of prematurity	High school	No
CB5	38	M	R	No	0	Detached retina	High school	Yes
CB6	31	F	R	No	0	Bilateral Retinoblastoma	High school	No
CB7	26	M	R	No	0	Leber's congenital amaurosis	University	Yes
CB8	30	M	R	No	0	Bilateral retinoblastoma	High school	Yes
CB9	46	M	R	No	0	Congenital Cataract	University	Yes
CB10	40	M	R	No	0	Retinopathy of prematurity	University	Yes
CB11	27	F	R	No	0	Retinopathy of prematurity	High school	No

Handedness was evaluated using an adapted version of the Edinburgh inventory (1). CB and SI were classified as "musician" if they currently practice or have practiced an instrument or vocal for more than 2 y on a regular basis (at least 2 h a week). M, male; F, female; R, right handed; L, left handed; A, ambidextrous.

1. Oldfield RC (1971) The assessment and analysis of handedness: The Edinburgh inventory. *Neuropsychologia* 9:97–113.

Table S5. Brain activations ($P < 0.001$, uncorrected) related to the main effects observed in our tasks

Area	Cluster size	*x* (mm)	*y* (mm)	*z* (mm)	*Z*
Task effect [Spatial > Pitch]					
Sighted					
R inferior parietal lobule	426	68	−32	38	4.27
	—	62	−42	48	3.89
	—	52	−40	32	3.85
R precentral gyrus	64	32	0	48	3.53
R middle occipito-temporal gyrus	28	48	−54	10	3.50
R middle frontal gyrus	15	34	60	8	3.25
Blind					
R middle occipital gyrus	3,179	50	−52	6	5.22*
	—	50	−64	10	4.78*
	—	12	−80	22	4.11
R inferior parietal lobule	283	36	−40	40	3.94
R superior frontal gyrus	43	24	10	68	3.72
R middle frontal gyrus	254	34	2	52	3.66
	—	46	−2	52	3.38
R lingual gyrus	68	24	−66	−2	3.33
Task effect [Pitch > Spatial]					
Sighted					
R central sulcus	128	58	−10	50	4.67*
R posterior superior temporal gyrus	287	46	−30	−6	4.45
R anterior inferior temporal cortex	171	44	−4	−32	3.96
L insula	647	−42	−24	22	3.96
L putamen	—	−20	6	10	3.56
L inferior frontal gyrus (opercular part)	61	−58	−8	16	3.74
L middle/superior temporal gyrus	221	−52	−36	4	3.73
R cerebellum	31	28	−72	−34	3.43
L cerebellum	20	−26	−54	−18	3.35
Blind					
No significant responses					
Group effect [Blind > Sighted]					
Spatial					
R lateral occipital gyrus	11,950	32	−80	−2	6.06*
L calcarine	—	−6	−86	6	4.96*
R lateral occipital gyrus	—	46	−64	8	4.70*
Pitch					
L calcarine	5,474	−6	−84	2	4.95*
L superior occipital gyrus	—	−20	−78	30	4.90*
R lateral occipital gyrus	—	26	−82	4	4.73*
Group effect [Sighted > Blind]					
Spatial					
R middle temporal gyrus	58	64	−8	−14	4.43
R hippocampus	67	24	−22	−10	4.05
R angular gyrus	202	50	−62	38	3.95
Pitch					
R angular gyrus	50	46	−64	46	4.16
R hippocampus	12	26	−40	−4	3.26
Main effects separately					
Spatial in sighted					
L premotor/motor cortex	5,924	−34	−10	52	5.69*
R superior temporal gyrus (A1)	1,119	66	−26	12	5.14*
R cerebellum	939	12	−72	20	5.05*
L superior temporal gyrus (A1)	903	−64	−18	12	4.3
R cerebellum	116	22	−62	−50	4.02
L cerebellum	68	−24	−64	−50	3.66
L cerebellum	132	−28	−64	−26	3.66
L inferior parietal lobule	12	−48	−38	56	3.27
Pitch in sighted					
L premotor/motor cortex	7,081	−6	8	54	5.88*
R cerebellum	1,607	34	−64	26	5.17*
R superior temporal gyrus (A1)	1,227	64	−26	10	5.11*
R inferior frontal gyrus	387	58	14	20	4.56
R precentral gyrus	399	56	2	48	4.31

Table S5. Cont.

Area	Cluster size	*x* (mm)	*y* (mm)	*z* (mm)	*Z*
R cerebellum	113	22	−64	−50	3.95
L cerebellum	165	−28	−62	−24	3.75
L thalamus/putamen	247	−14	−16	6	3.68
L cerebellum	12	−22	−64	−50	3.23
Spatial in blind					
L cuneus/primary visual cortex (V1)	14,966	−6	−86	6	6.27*
L premotor/motor cortex	8,929	−34	−10	52	5.86*
L intraparietal sulcus	—	−38	−42	48	5.15*
R superior temporal gyrus (A1)	1,561	64	−26	10	5.69*
L superior temporal gyrus (A1)	1,511	−60	−32	12	4.96*
R intraparietal sulcus	398	42	−40	44	4.36
R superior frontal gyrus	181	38	38	28	4.06
L brainstem	21	−6	−22	−8	3.81
R superior parietal lobule	98	30	−56	54	3.45
R brainstem	5	6	−22	−10	3.33
Pitch in blind					
L cuneus/primary visual cortex (V1)	10,453	−6	−84	4	6.26*
L premotor/motor cortex	7,581	−12	−2	62	6.08*
R superior temporal gyrus (A1)	1,624	64	−26	10	5.89*
L superior temporal gyrus (A1)	1,884	−58	−32	12	5.66*
L occipito-temporal gyrus	532	−44	−62	6	4.54
R occipito-temporal gyrus	252	46	−60	6	4.48
R insula	251	32	20	6	4.2
R inferior frontal gyrus	463	58	12	8	4.11
R intraparietal sulcus	81	42	−36	42	3.6
R superior frontal gyrus	22	36	38	28	3.48
L thalamus	26	−14	−16	6	3.39

*Significant after correction over the entire volume at $P < 0.05$.